Direct Regulation of BK Channels by Phosphatidylinositol 4,5-Bisphosphate as a Novel Signaling Pathway

Thirumalini Vaithianathan,[1] Anna Bukiya,[1] Jianxi Liu,[1] Penchong Liu,[1] Maria Asuncion-Chin,[1] Zheng Fan,[2] and Alejandro Dopico[1]

[1]Department of Pharmacology and [2]Department of Physiology, The University of Tennessee Health Science Center, Memphis, TN 38163

Large conductance, calcium- and voltage-gated potassium (BK) channels are ubiquitous and critical for neuronal function, immunity, and smooth muscle contractility. BK channels are thought to be regulated by phosphatidylinositol 4,5-bisphosphate (PIP_2) only through phospholipase C (PLC)–generated PIP_2 metabolites that target Ca^{2+} stores and protein kinase C and, eventually, the BK channel. Here, we report that PIP_2 activates BK channels independently of PIP_2 metabolites. PIP_2 enhances Ca^{2+}-driven gating and alters both open and closed channel distributions without affecting voltage gating and unitary conductance. Recovery from activation was strongly dependent on PIP_2 acyl chain length, with channels exposed to water-soluble diC4 and diC8 showing much faster recovery than those exposed to PIP_2 (diC16). The PIP_2–channel interaction requires negative charge and the inositol moiety in the phospholipid headgroup, and the sequence RKK in the S6–S7 cytosolic linker of the BK channel-forming (cbv1) subunit. PIP_2-induced activation is drastically potentiated by accessory β_1 (but not β_4) channel subunits. Moreover, PIP_2 robustly activates BK channels in vascular myocytes, where β_1 subunits are abundantly expressed, but not in skeletal myocytes, where these subunits are barely detectable. These data demonstrate that the final PIP_2 effect is determined by channel accessory subunits, and such mechanism is subunit specific. In HEK293 cells, cotransfection of cbv1+β_1 and PI4-kinaseIIα robustly activates BK channels, suggesting a role for endogenous PIP_2 in modulating channel activity. Indeed, in membrane patches excised from vascular myocytes, BK channel activity runs down and Mg-ATP recovers it, this recovery being abolished by PIP_2 antibodies applied to the cytosolic membrane surface. Moreover, in intact arterial myocytes under physiological conditions, PLC inhibition on top of blockade of downstream signaling leads to drastic BK channel activation. Finally, pharmacological treatment that raises PIP_2 levels and activates BK channels dilates de-endothelized arteries that regulate cerebral blood flow. These data indicate that endogenous PIP_2 directly activates vascular myocyte BK channels to control vascular tone.

INTRODUCTION

Blood circulation depends on the myogenic tone of small, resistance-size arteries (Meininger and Davis, 1992). While myogenic tone is regulated by endothelial, neuronal, and circulating factors, it is ultimately determined by the activity of ion channels and signaling molecules in the myocyte itself (Faraci and Heistad, 1998). Tone is increased by a rise in overall cytosolic calcium (Ca^{2+}_i) in the myocyte, which can be achieved by Ca^{2+} influx via depolarization-activated Ca^{2+} channels in the cell membrane and/or Ca^{2+} release from intracellular stores (Jaggar, 2001). Depolarization and increases in Ca^{2+}_i lead to activation of large-conductance, Ca^{2+}/voltage-gated K^+ (BK) channels, which generate outward currents that tend to hyperpolarize the membrane and thus close voltage-gated Ca^{2+} channels. Therefore, BK channel activation limits voltage-dependent Ca^{2+} entry and myocyte contraction (Brayden and Nelson, 1992; Jaggar et al., 2005).

Phosphatidylinositol 4,5–bisphosphate (PIP_2) plays a key role as an intermediate molecule in many receptor-mediated signaling pathways, including those regulating myocyte contraction (Tolloczko et al., 2002). PIP_2 hydrolysis by PLC renders 1,4,5-trisphosphate (IP_3) and diacylglycerol (DAG) (Nahorski et al., 1994). IP_3 mobilizes sarcoplasmic Ca^{2+}, while DAG activates PKC. Mobilized Ca^{2+} and activated PKC eventually regulate myocyte BK channel activity (Jaggar et al., 1998; Jaggar, 2001). It is thought that, by producing IP_3 and DAG, PIP_2 indirectly modulates BK channels, and thus myocyte contraction. However, PIP_2 also acts as a signaling molecule

Correspondence to Alex Dopico: adopico@utmem.edu

The online version of this article contains supplemental material.

Abbreviations used in this paper: BK, Ca^{2+}/voltage-gated K^+; C/A, cell-attached; DAG, diacylglycerol; DOG, 1,2-dioctanoyl-sn-glycerol; FA, fatty acids; GPCR, Gq-coupled receptor; HEDTA, 1.6 N-(2-hydroxyethyl)-ethylenediamine-triacetic acid; I/O, inside-out; IP_3, 1,4,5-trisphosphate; OA, okadaic acid; O/O, outside-out; PC, 1,2-dipalmitoyl-*sn*-glycero-3-phosphocholine; PIP_2, phosphatidylinositol 4,5-bisphosphate; PPI, phosphoinositide; PS, 1,2-dipalmitoyl-*sn*-glycero-3-phospho-L-serine; PSS, physiological saline solution; RT, reverse transcription; SR, sarcoplasmic reticulum; 4-AP, 4-aminopyridine.

The Rockefeller University Press $30.00
J. Gen. Physiol. Vol. 132 No. 1 13–28
www.jgp.org/cgi/doi/10.1085/jgp.200709913

on its own through direct interaction with target proteins. In particular, PIP_2 directly modulates the activity of ion channels and transporters (Hilgemann and Ball, 1996; Fan and Makielski, 1997; Runnels et al., 2002; Rohács et al., 2003; Chemin et al., 2005; Suh and Hille 2005; Brauchi et al., 2007; Hilgemann, 2007; Rohács 2007; Voets and Nilius, 2007). In spite of the key roles of PIP_2 and BK channels in cell excitability and signaling, it remains unknown whether PIP_2 can directly modulate BK channel function.

Here, we demonstrate that PIP_2 directly (i.e., independently of PIP_2 metabolites and downstream signaling) increases BK channel steady-state activity, the pore-forming (cbv1) subunit being sufficient to sense the phosphoinositide (PPI). The cbv1–PIP_2 interaction requires recognition of negative charges and the inositol moiety in the PIP_2 headgroup by a channel sequence that meets major criteria for a PIP_2 binding site. This interaction results in a drastic increase in the channel's apparent Ca^{2+} sensitivity, with changes in both open and closed time distributions. PIP_2 action on cbv1 channels is drastically amplified by coexpression of the smooth muscle–abundant, channel accessory β_1, but not other (e.g., β_4), subunit. PIP_2 robustly activates native BK channels in vascular myocytes where β_1 is highly expressed, but not in skeletal myocytes, where β_1 is barely detected. Using intact vascular myocytes under physiological conditions of Ca^{2+} and voltage, we demonstrate that endogenous PIP_2 plays a role in activating BK channels via the direct mechanism. Furthermore, manipulation of endogenous PIP_2 levels dilates pressurized, resistance-size cerebral arteries, an effect that is prevented by selective BK channel block.

MATERIALS AND METHODS

Cerebral Artery Diameter Measurement and Myocyte Isolation

Sprague-Dawley rats (250 g) were decapitated, and middle cerebral and basilar arteries were isolated. Following endothelium removal and artery pressurization (Liu et al., 2004), vessels were extralumenally perfused with physiological saline solution (Liu et al., 2004) at 3.75 ml/min using a peristaltic pump (Rainin Dynamax RP-1). Drug stock solutions (see below) were diluted in PSS to final concentration. Diameter changes were determined with IonWizard 4.4 (IonOptics).

Single myocytes were isolated from cerebral arteries following procedures already described (Liu et al., 2004; Bukiya et al., 2007). Skeletal muscle fibers were prepared using slight modifications to methods described elsewhere (McKillen et al., 1994). In brief, flexor digitorum brevis muscle was dissected from adult Sprague-Dawley rats and incubated in 0.3% collagenase (Type 1) in Ringer solution (in mM): 146.3 NaCl, 4.75 KCl; 1 $CaCl_2$; 0.95 Na_2HPO_4, 0.5 $MgCl_2$; 9.5 HEPES, adjusted to pH 7.4 with NaOH. Muscles were incubated in this solution at 4°C for 30 min and switched to 37°C for 90 min. Single fibers were isolated in Ringer solution without collagenase by triturating the tissue with fire-polished Pasteur pipettes. The isolated fibers were then placed in a solution containing (in mM) 139 KCl, 5 EGTA, 10 HEPES, adjusted to pH 7.4 with KOH. In this solution, sarcolemmal vesicles formed on the surface of the muscle fibers.

Mutagenesis and cRNA Injection

cDNA encoding cbv1 was cloned using PCR and reverse transcription (RT) from total RNA of myocytes freshly isolated from rat small cerebral arteries (Quinn et al., 2003; Jaggar et al., 2005). The pOX vector and full-length cDNAs coding for BK β_1 and β_4 were gifts from A. Wei (Washington University at St. Louis, St. Louis, MO), M. Garcia (Merck Research Laboratories, Rahway, NJ), and L. Toro (University of California at Los Angeles, Los Angeles, CA). We used Quickchange (Stratagene) to mutate RKK in the cbv1 S6–S7 linker. Sequencing was conducted at the University of Tennessee Molecular Research Center. cDNA coding for cbv1 was cleaved with BamHI (Invitrogen) and XhoI (Promega) and inserted into pOX. pOX-cbv1 and pOX-RKKcbv1AAA were linearized with NotI and SacII (Promega) and transcribed in vitro using T3. PBScMXT-K239cbv1A was linearized by SalI and transcribed in vitro using T3. BK β_1 cDNA inserted into pCI-neo was linearized with NotI and transcribed in vitro using T7. BK β_4 cDNA inserted into pOx was linearized with NotI and transcribed using T3. The mMessage-mMachine kit (Ambion) was used for transcription.

Oocytes were removed from *Xenopus laevis* and prepared as previously described (Dopico et al., 1998). cRNA was dissolved in DEPC-treated water at 5 (cbv1) and 15 (β_1 or β_4) ng/μl; 1-μl aliquots were stored at −70°C. Cbv1 cRNA was injected alone (2.5 ng/μl) or coinjected with β_1 or β_4 (7.5 ng/μl) cRNAs, giving molar ratios ≥6:1 (β:α) (Bukiya et al., 2007). Expression of the mutated cbv1 was lower than that of wild type (wt); thus, cRNA was increased to 3 μg/μl for a total volume of 23 nl. After cRNA injection, oocytes were prepared for patch-clamping as previously described (Dopico et al., 1998).

Cell Culture and Transfection

HEK-293 cells were transfected with pcDNA3 vector-cbv1 cDNA and pC1-Neo vector-β_1 cDNA with or without pCMV5 vector-PI4KIIα cDNA. Transfection was performed with Lipofectamine 2000 (Invitrogen).

Electrophysiology

Currents were acquired using an EPC8 amplifier (List), low-passed at 1 kHz with an 8-pole Bessel filter (Frequency Devices), and digitized at 10 kHz using 1320 Digidata/pClamp8 (Molecular Devices). Data from single channel patches for dwell-time analysis were acquired at 7 kHz and digitized at 35 kHz. Patch pipettes were prepared as described elsewhere (Dopico et al., 1998). Experiments were performed at room temperature. Solutions were made with deionized (18 MΩ.cm) water and high-grade purity salts. Free Ca^{2+} concentrations were calculated using Max Chelator Sliders (C. Patton, Stanford University, Stanford, CA) and validated experimentally (Dopico, 2003). A variety of solutions were used, as follows.

Perforated-Patch Experiments on Vascular Myocytes. The pipette solution contained (in mM) 110 K-aspartate, 30 KCl, 10 NaCl, 1 $MgCl_2$, 10 HEPES, and 0.05 EGTA, with pH adjusted to 7.2 by adding KOH. The perforated-patch configuration was achieved by adding amphotericin B dissolved in DMSO into pipette solution at a concentration of 250 μg/ml. Myocytes were bathed in HEPES-buffered physiological saline (PSS). PSS had the following composition (in mM): 134 NaCl, 6 KCl, 2 $CaCl_2$, 1 $MgCl_2$, 10 HEPES, and 10 glucose, with pH adjusted to 7.4 by adding NaOH.

Excised Patch Recordings from Vascular Myocytes. For inside-out (I/O) recordings, the electrodes were filled with (in mM) 130 KCl, 5.22 $CaCl_2$, 2.28 $MgCl_2$, 15 HEPES, 5 EGTA, and 1.6 N-(2-hydroxyethyl)-ethylenediamine-triacetic acid (HEDTA), with pH

adjusted to 7.4 by adding KOH and a free $[Ca^{2+}] \approx 10$ μM. The bath solution contained (in mM) 130 KCl, 3.84 $CaCl_2$, and 1 $MgCl_2$, 15 HEPES, and 5 EGTA, with pH adjusted to 7.4 by adding KOH and a free $[Ca^{2+}] \approx 0.3$ μM. For outside-out (O/O) recordings, the electrode and bath solution correspond to the bath and electrode solution used in I/O recordings. For cell-attached (C/A) recordings, the electrode solution contained (in mM) 127 NaCl, 3 KCl, 1.8 $CaCl_2$, 2 $MgCl_2$, 15 HEPES, pH 7.4. This physiological K^+ gradient sets E_K at −97 mV. The bath solution contained (in mM) 130 KCl, 2.97 $CaCl_2$, 1 $MgCl_2$, 5 EGTA, 15 HEPES, with pH adjusted to 7.4 by adding KOH and a free $[Ca^{2+}] \approx 0.1$ μM.

Rundown Experiments from Vascular Myocyte I/O Patches. The electrodes and bath contained the same solution (in mM) 130 KCl, 4.94 $CaCl_2$, 2.44 $MgCl_2$, 15 HEPES, 5 EGTA, and 1.6 HEDTA, with pH adjusted to 7.4 by adding KOH; free $[Ca^{2+}] \approx 3$ μM. Immediately after excision, I/O currents were recorded at 0, 3, 10, and 30 min. After 30 min (maximal rundown; Lin et al., 2005), the BK channel was reactivated with Mg-ATP (0.5 mM) together with okadaic acid (OA, 2 nM) (Lin et al., 2005). PIP_2 monoclonal antibodies (1:1,000, Assay Designs) were applied to the cytosolic side of the membrane.

Skeletal Muscle BK Channel Recordings. Membrane patches were excised from isolated skeletal muscle fibers, and BK currents were recorded in the I/O configuration by using techniques similar to those described for vascular myocyte I/O recordings. The bath solution, however, contained (in mM) 130 KCl, 5.22 $CaCl_2$, 2.28 $MgCl_2$, 15 HEPES, 5 EGTA, and 1.6 HEDTA, with pH adjusted to 7.4 by adding KOH; free $[Ca^{2+}] \approx 10$ μM.

Oocyte Recordings. Oocytes were isolated from *X. laevis* and treated for patch-clamp recordings as mentioned in the text and described in detail elsewhere (Dopico et al., 1998). Recordings were performed in the I/O configuration; the electrode and bath solutions had compositions similar to the electrode and bath solutions used in myocyte experiments (see above), except that K-gluconate replaced KCl to avoid contaminating recordings with endogenous Ca^{2+}-activated Cl^- channel activity (Dopico et al., 1998). In this series of experiments, bath $[Ca]^{2+}$ was set to 0.3 or 10 μM by changing the amount of $CaCl_2$ and EGTA buffer.

Experiments on Transfected HEK Cells. Cells were transfected and cultured as described above. Recordings were obtained in the I/O configuration. The bath solution contained (in mM) 5 Na^+gluconate, 140 K^+gluconate, 1 $MgCl_2$, 15 HEPES, 0–4 HEDTA, 0–4 EGTA, and 0.43–2.2 $CaCl_2$, pH adjusted to 7.35 with KOH. The concentrations of $CaCl_2$, EGTA, and HEDTA were adjusted to obtain the desired concentrations of free metal as described above. The electrode solution contained (in mM) 140 K^+gluconate, 1 $MgCl_2$, 2.2 mM $CaCl_2$, 15 HEPES, 4 HEDTA, and 4 EGTA. Cells were washed for 30 min in 2.2 mM Ca^{2+} bath solution before recordings. Single channel records were obtained as explained above for oocytes and myocytes.

Voltage Protocols and Data Analysis. For perforated-patch recordings in myocytes, the membrane was held at −80 mV, and total outward currents were evoked by 0.2-s, 20-mV depolarizing steps from −60 to 100 mV; leak currents were determined using a P/4 protocol. Peak current amplitude was determined 0.14–0.19 s after the start of the pulse and obtained after digital subtraction of leak from total current. For macroscopic excise patch recordings in oocytes, the membrane was held at 0 mV, and total outward currents were evoked by 0.2-s, 10-mV depolarizing steps from −100 to 200 mV. Peak current amplitude was determined 0.14–0.19 s after the start of the pulse.

As index of channel steady-state activity, we used the product of the number of channels present in the membrane patch (N) and the channel open probability (P_o). NP_o was calculated from all-points amplitude histograms (Dopico et al., 1998). At the beginning of each experiment, NP_o was determined from ≥5 min to ensure that changes in activity at the time of reagent application were due to the reagent itself and not to nonstationary NP_o. NP_o under a given condition was obtained from >3 min of continuous recording. Dwell time analysis was conducted as previously described (Dopico et al., 1998; Crowley et al., 2003). Channel mean open time (t_o) in multichannel patches of unknown N was obtained from $t_o = NP_o\ T/\#o$; where $\#o$ is the number of channel openings during several minutes (T) of continuous current recording under each condition (Fenwick et al., 1982; Dopico et al., 1998). Data and idealized records were analyzed using pClamp 9.2 (Molecular Devices) as described elsewhere (Dopico et al., 1998) and plotted and fitted using Origin 6.1 (Origin Laboratory).

Compounds and their Application

Stock solutions of anionic phospholipids (PS [synthetic], PI [synthetic, Echelon Biosciences], PI5P [synthetic], PIP_2 [diC16, synthetic, Calbiochem and Sigma-Aldrich], PIP_3 [synthetic]) were made in ultrapure distilled water at a lipid concentration of 10 μM by sonication on ice for 30 min immediately before the experiment. PC (semisynthetic), a switterionic phospholipid, was first dissolved in pure DMSO at a concentration of 2 mM and then mixed and sonicated for 30 min in recording solution to obtain a final lipid concentration of 10 μM. Dibutanoyl and dioctanoyl PIP_2 (synthetic, Sigma-Aldrich) (diC4 and diC8) were diluted in ultrapure distilled water at a lipid concentration of 10 μM. The lipid-containing solutions were applied to the cytosolic side of the patch membrane immediately after the dispersal procedure. For the O/O and whole-cell recordings, lipid-containing solutions were applied to the external side of the membrane. For the C/A recordings, lipid-containing solutions were applied to the extracellular, extrapatch surface of the cell.

Poly-L-lysine was dissolved in high-purity deionized water (50 mg/ml stock), further diluted in bath solution to 100 μg/ml, and applied to the cytosolic side of I/O patches. 1,2-dioctanoyl-sn-glycerol (DOG) was dissolved in DMSO (1 mg/ml stock), further diluted in bath solution to 2 μM, and applied to the cytosolic side of I/O patches. Before recording changes in channel activity evoked by a given compound, control recordings were obtained when a steady-state perfusion was achieved, which typically took 5–10 min.

For the perforated-patch recordings, agent-containing solutions were applied to the extracellular, extrapatch surface of the cell. Ro 31-8220 (Biomol Research Laboratories) was reconstituted in DMSO stock (10 μg/ml) and diluted in bath solution to a final concentration of 2 μM. Thapsigargin was reconstituted in DMSO stock (10 mM) and diluted in bath solution to a final concentration of 200 nM. Paxilline was dissolved in DMSO as a 23 mM stock and further diluted in bath solution to a final concentration of 300 nM. Wortmannin (Stressgen Bioreagents) was reconstituted in DMSO stock (50 mg/ml) and diluted in bath solution to a final concentration of 5 nM. U73122 (Biomol Research Laboratories) was reconstituted in DMSO stock (4 mM) and diluted to a final concentration of 5–25 μM. 4-aminopyridine (4-AP) was dissolved in high-purity deionized water as a 0.8 M stock and further diluted in bath solution to a final concentration of 5 mM. 2-[[3-(trifluoromethyl)phenyl] amino]pyridine-3-carboxylic acid (niflumic acid) was dissolved in acetone as a 0.2 M stock and further diluted in bath solution to a final concentration of 100 μM.

Compounds applied to pressurized vessels were diluted to make stock solutions as described above and then further diluted in PSS to final concentration. Unless otherwise stated, all compounds were purchased from Sigma-Aldrich.

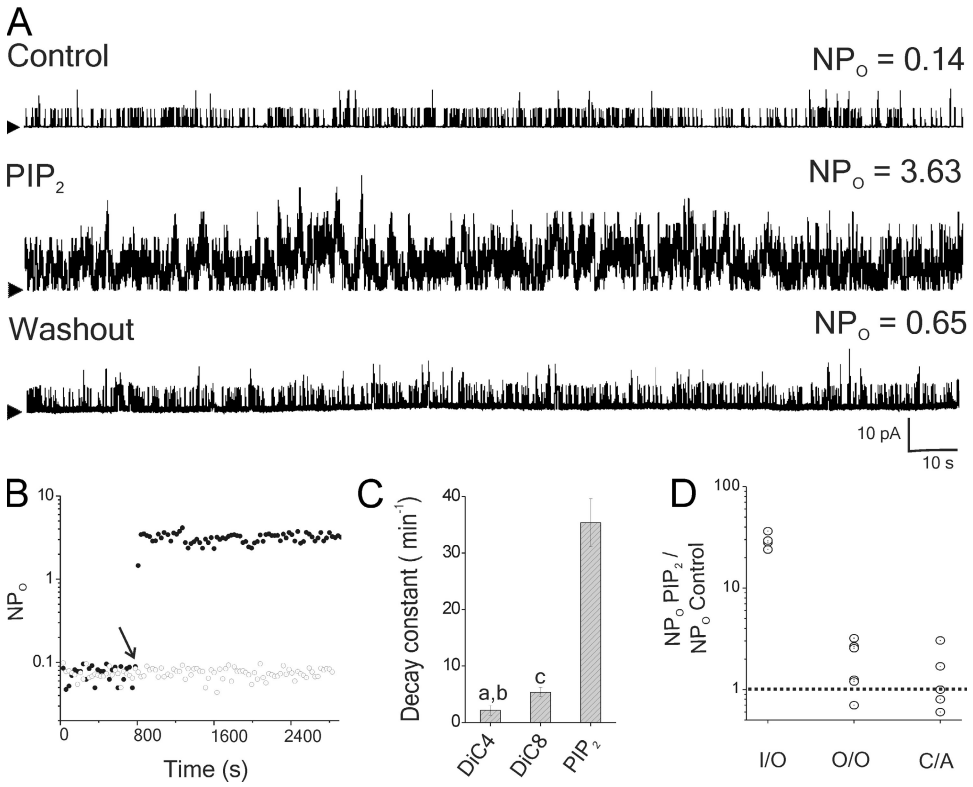

Figure 1. PIP_2 readily activates myocyte BK channels when accessing the channel from the inner membrane leaflet. (A) Unitary currents obtained before (top), after a 5-min bath application of 10 μM PIP_2 (diC16) (middle), and after washout for >30 min (bottom) of I/O patches. Arrowheads, baseline; upward deflections, channel openings; $n = 5$. (B) Steady-state activity (NP_o) time course from two I/O patches. An arrow highlights the time at which one of the patches (●) was switched from control to PIP_2-containing solution. The other patch was continuously exposed to control (○). (C) Kinetics of reversibility of diC4, diC8, and PIP_2 action. Decay constant values were obtained by single exponential fittings of NP_o vs. time plots. (a) diC4 vs. diC8: $P < 0.001$; (b) diC4 vs. diC8: $P < 0.001$; (c) diC8 vs. PIP_2: $P < 0.001$, $n = 3$–4. In A and B, V = 40 mV, Ca^{2+}_i = 0.3 μM; $n = 3$. (D) NP_o responses to 10 μM PIP_2 from I/O, O/O, and C/A patches. Each point = one patch/myocyte. Dotted line, control; V = 10–60 mV; Ca^{2+}_i = 0.3 μM; $n = 4$–6.

Online Supplemental Material

The online supplemental material (available at http://www.jgp.org/cgi/content/full/jgp.200709913/DC1) contains one figure showing both representative unitary current recordings and averaged channel activity data in response to application of 10 μM PIP_3 to the cytosolic side of inside-out patches from *Xenopus laevis* oocytes that express wt cbv1, RKKcbv1AAA, or K239cbv1A. Results show that the PIP_3 responses in the K239A mutant are similar to those in wt cbv1, while RKKcbv1AAA responses are significantly blunted, indicating that the RKKcbv1AAA mutation in the cbv1 S6–S7 linker distinctly reduces PIP_3 activation of cbv1 channels.

RESULTS

PIP_2 Activates BK Channels in Cerebral Artery Myocytes

We first applied PIP_2 to the cytosolic side of I/O patches excised from freshly isolated myocytes and determined responses in channel steady-state activity (NP_o; see Materials and methods). Studies were conducted with $Ca^{2+}_i \approx 0.3$ μM, which is found in cerebral artery myocytes (Knot and Nelson, 1998; Pérez et al., 2001). The membrane potential was held positive to evoke an easily measurable NP_o. PIP_2 at levels found in plasma membranes (10 μM; McLaughlin and Murray, 2005) increased NP_o (5/5 cells) (Fig. 1 A), reaching 2,831 ± 202% of control. In submicromolar concentrations of Ca^{2+}_i, PIP_2-induced increase of BK NP_o was sustained, persisting ~30 min after PIP_2 application (Fig. 1 B) and returning to pre-PIP_2 values after washout in bath solution for >30 min (Fig. 1 A). These data suggest that the increase in BK NP_o is due to PIP_2 itself, instead of PIP_2 active metabolites.

The more water-soluble diC4 and diC8 analogues also readily increased BK NP_o ($n = 4$; V= +40 mV), with NP_o readily turning to preanalogue values with wash in bath solution. The diC4 and diC8 effect, however, differed from that of PIP_2 in two aspects. First, the potentiation of channel activity was much more robust for PIP_2 than those caused by the two more soluble analogues: 2,831 ± 202, 308 ± 56, and 230 ± 34% of control for PIP_2, diC8, and diC4, respectively. As discussed with inward rectifier K^+ channels (Rohács et al., 1999; Cho et al., 2006), the increased effectiveness of PIP_2 in potentiating BK NP_o likely reflects the increased partition of this hydrophobic analogue in the lipid environment and, eventually, more effective loading of the cell membrane with increased access to the channel target. Second, recovery from potentiation was much faster for diC4 and diC8 (Fig. 1 C). Conceivably, the fast relaxation of these analogues reflects elimination of bound diC4/diC8 monomers from a binding site(s) that is readily accessible from the aqueous phase. In contrast to diC4 and diC8, lipids with longer side chains such as PIP_2 are not only in monomeric but also (and mainly) in micellar

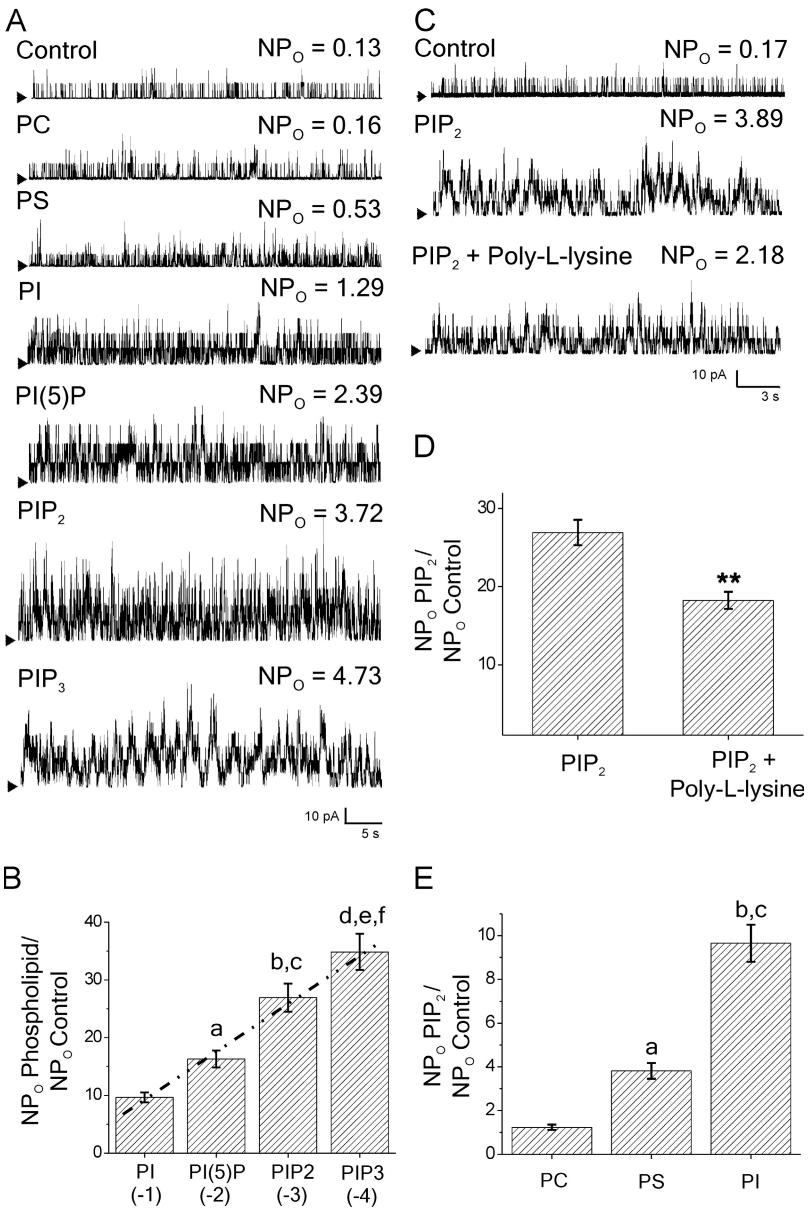

Figure 2. Negative charge and inositol moiety both contribute to phosphoinositide activation of myocyte BK channels. (A) Unitary currents from I/O patches exposed to control or phospholipids that differ in headgroup structure. Arrowheads, baseline; upward deflections, channel openings. (B) BK channel potentiation is a direct function (r = 0.99) of negative charge in the phospholipid headgroup. (a) PI vs. PI5P: $P < 0.001$; (b) PI vs. PIP_2: $P < 0.001$; (c) PI5P vs. PIP_2: $P < 0.001$; (d) PI vs. PIP_3: $P < 0.001$; (e) PI5P vs. PIP_3: $P < 0.001$; (f) PIP_2 vs. PIP_3: $P < 0.05$; $n = 3$–12. (C) I/O recordings and (D) averaged data show that coapplication of 0.1 mg/ml poly-L-lysine reduces PIP_2 activation of BK channels; $n = 3$. (E) PS and PI (net charge ≈ −1) cause more robust activation than that evoked by the neutral PC. However, PI is more effective than PS. (a) PC vs. PS: $P < 0.05$; (b) PC vs. PI: $P < 0.001$; (c) PS vs. PI: $P < 0.001$; $n = 3$–6. All phospholipid species had dipalmitoyl chains. V = 40 mV; $Ca^{2+}_i = 0.3$ μM.

form in the aqueous phase (Flanagan et al., 1997; Huang et al., 1998). Thus, PIP_2 micelles can incorporate into the bilayer to form mixed micelles. Release of these micelles from the membrane should take times much longer than those corresponding to bound-monomer dissociation from a target site, resulting in slower channel recovery from activation (Rohács et al., 1999).

The increased NP_o caused by PIP_2 application was not accompanied by any noticeable change in unitary current amplitude (Fig. 1 A). Slope unitary conductance remained constant in the presence of PIP_2 when evaluated across a voltage range at which the current was ohmic (−60 to 40 mV in 1 mM Mg^{2+}_i and symmetric 130 mM K^+: 243 vs. 251 pS, control and PIP_2). Thus, within this voltage range, any PIP_2 modification of macroscopic current should be attributed to PIP_2 action on NP_o.

Because PIP_2 effects on NP_o were recorded in cell-free patches (even >20 min after excision) in a highly buffered Ca^{2+} solution containing no nucleotides, it is unlikely that cytosolic messengers mediate PIP_2 action. Rather, PIP_2 targets the BK channel itself, its proteolipid microenvironment, or a lipid–protein interface. In contrast to I/O results, PIP_2 failed to consistently increase NP_o when applied to the extra-patch membrane of C/A patches (Fig. 1 D). This is consistent with the difficulty that a charged molecule (charge ≈ −3 at physiological pH) may have in accessing a target located in the membrane within the pipette. The PIP_2 effect was also mild and inconsistent when the lipid was applied to the extracellular side of O/O patches (Fig. 1 D). The contrast between I/O and C/A or O/O results indicates that PIP_2 accesses its site of action most effectively from the

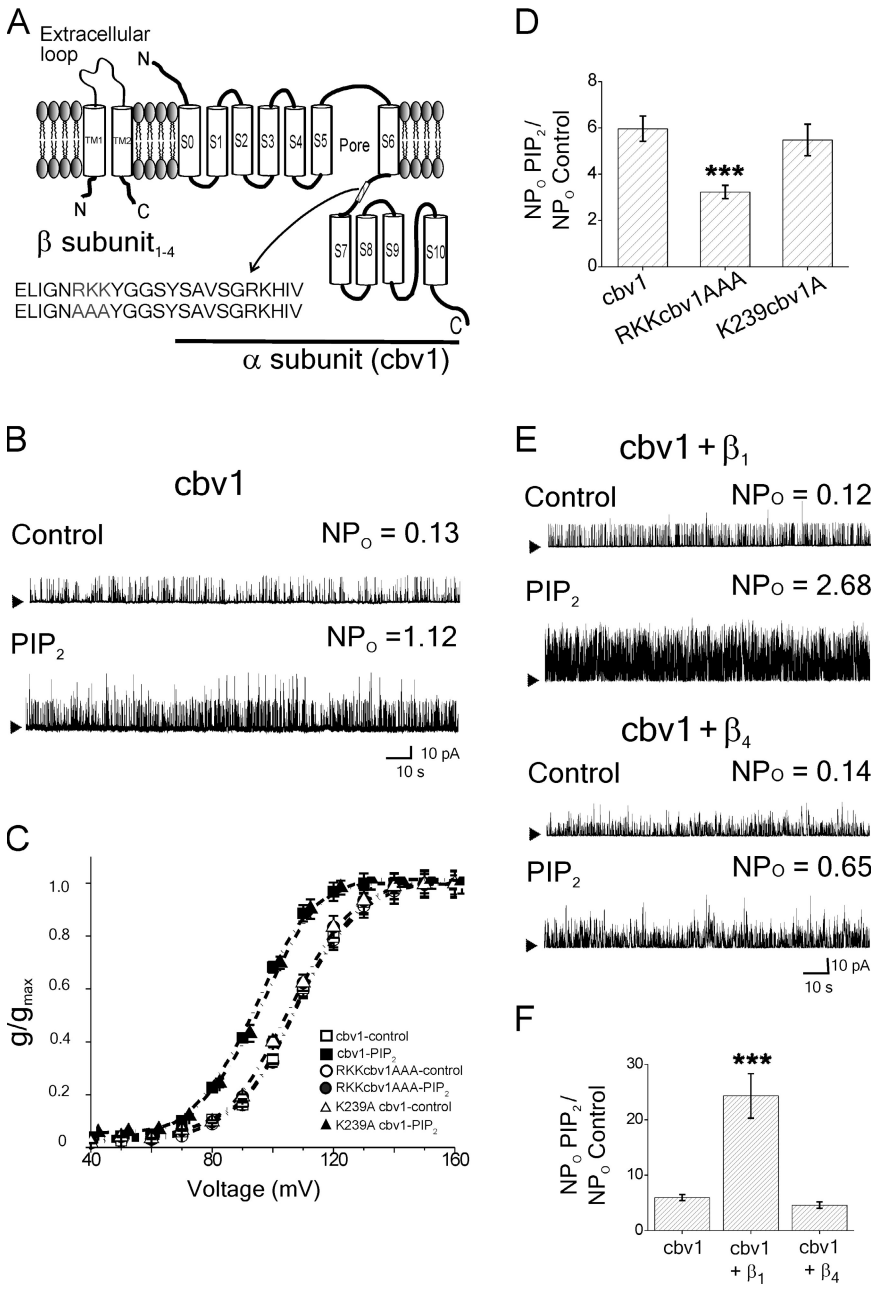

Figure 3. Cbv1 is sufficient to support PIP_2 action, which is amplified by β_1 (but not β_4) subunits. (A) BK channel dimer made of channel-forming (cbv1) and auxiliary $\beta_{(1-4)}$ subunits. The RKK to AAA mutation in the cbv1 S6–S7 linker is shown in bold. (B) Unitary currents from an I/O patch expressing cbv1 in the absence (top) and presence (bottom) of PIP_2. Arrowheads, baseline; upward deflections, channel openings. (C) Averaged G-voltage macroscopic current data fitted to Boltzmann functions from wt cbv1, RKKcbv1AAA, and K239cbv1A in the absence and presence of PIP_2; the lipid causes a parallel leftward shift in wt and K239cbv1A but not in the RKKcbv1AAA mutant; n = 4–6. (D) PIP_2-induced increase in NP_o is significantly reduced in the RKKcbv1AAA mutant when compared with wt cbv1 or the K239cbv1A mutant; ***, $P < 0.001$; n = 4. (E). Unitary currents from I/O patches coexpressing cbv1+β_1 (top) or cbv1+β_4 subunits (bottom) in the absence and presence of PIP_2. Arrowheads, baseline; upward deflections, channel openings. (F) Averaged PIP_2 responses of cbv1, cbv1+β_1, and cbv1+β_4; n = 4–6. For B and E, arrows, baseline. For A, B, and D–F, V = 40 mV; Ca^{2+}_i = 0.3 μM.

cytosolic side of the membrane, where PIP_2 is naturally predominant (Laux et al., 2000).

Structural Determinants of PIP_2 Action

Negative charges and the position of the phosphates in the inositol ring are important for phosphoinositide interaction with Kir channels (Suh and Hille, 2005). In addition, the BK channel displays higher P_o when reconstituted in lipid bilayers that include negatively charged phospholipids (Park et al., 2003). Thus, we next probed phospholipids having different negative charges in their headgroups. Because PIP_2 chain length modified the magnitude and time course of BK channel activation (see previous section), we used lipid species having the same acyl chains. Dipalmitoyl chains were chosen because their length mimics that of phospholipid acyl chains prevalent in natural membranes. When applied to the intracellular side of I/O patches, all phosphoinositides readily increased NP_o (Fig. 2 A). Moreover, channel activation correlated positively with the number of negative charges in the phospholipid headgroup: NP_o = 957, 1801%, 2831%, and 3629% of controls for D (+)-*sn*-1,2-dipalmitoylglyceryl, 3-*O*-phospho linked (PI) (−1), 1,2-dipalmitoyl-L-α-phosphatidyl-D-myo-inositol 5-monophosphate (PI5P) (−2), PIP_2 (−3), and 1,2-dipalmitoylphosphatidylinositol 3,4,5-trisphosphate (PIP_3) (−4) (Fig. 2 B).

Among all phosphoinositides tested, PIP_3 showed the highest effectiveness, whether evaluated in myocyte native

BK channels (NP_o = ~3,500% of control; Fig. 2 B) or cbv1 expressed in *X.* oocytes (NP_o = ~900% of control). From multichannel patches, we determined that PIP_3 raised the channel mean open time (t_o) from 0.39 to 0.51 ms. The increment in t_o (+31%) cannot account solely for the PIP_3-induced increase in P_o (~900%). Therefore, the drastic increase in P_o in response to PIP_3 must be attributed to a combination of mild increase in t_o and robust increase in frequency of channel openings (i.e., a decrease in channel mean closed time; Dopico et al., 1998), the latter being evident in the traces shown in Fig. S1 A.

Adding the polycationic PIP_2 scavenger poly-L-lysine to the bath solution (0.1 mg/ml) (Quinn et al., 2003) significantly reduced PIP_2 action: NP_o in PIP_2 reached only 975% of controls in the presence of poly-L-lysine, in contrast to the 2,831% of control obtained in the same patch when recorded in poly-L-lysine–free solution (Fig. 2 C). Poly-L-lysine itself, however, usually failed to readily (<3 min) modify NP_o (unpublished data). Thus, poly-L-lysine's blunting of PIP_2 action appears not to result from opposite modulation of NP_o by the polycation and the negatively charged lipid. After 3 min of poly-L-lysine application, BK NP_o did decrease significantly (−35 ± 1.4%; n = 3). Collectively, results with poly-L-lysine are interpreted as the polycation scavenging PIP_2 via salt bridges formed between the positive charges of the former and the negative headgroup of the latter. Finally, 1,2-dipalmitoyl-*sn*-glycero-3-phosphocholine (PC), a phospholipid with no net charge at physiological pH (i.e., our recording conditions), barely increased NP_o (Fig. 2 E). Collectively, data indicate that the amount of negative charge in the phospholipid headgroup is a key determinant for PIP_2 and analogues to activate arterial myocyte BK channels.

We next examined whether the specific structure of the headgroup contributes to phosphoinositide action on the BK channel by probing PI vs. 1,2-dipalmitoyl-*sn*-glycero-3-phospho-L-serine (PS). Both phospholipids carry the same net charge (−1) under our recording conditions, but differ in their headgroup base (inositol vs. serine). PI increased NP_o to 957% of control, which is substantially greater than that caused by PS (NP_o = 356% of control) ($P < 0.001$) (Fig. 2 E). Therefore, added to the negative charge, the inositol moiety favors channel activation. This structural specificity is consistent with the idea that phosphoinositides target a defined protein site.

Cbv1 Is Sufficient for PIP_2 Action, which Is Drastically Amplified by β_1, but Not β_4, Subunits

Cerebrovascular myocyte BK channels consist of pore-forming α (cbv1, encoded by *KCNMA1*) and accessory β_1 (*KCNMB1*) subunits (Orio et al., 2002; Jaggar et al., 2005; Liu, J., P. Liu, M. Asuncion-Chin, and A. Dopico. 2005. *Soc. Neurosci. Abstr. Online.* 960:913) (Fig. 3 A). After cbv1 expression in *Xenopus* oocytes, application of PIP_2 to the cytosolic side of I/O patches consistently

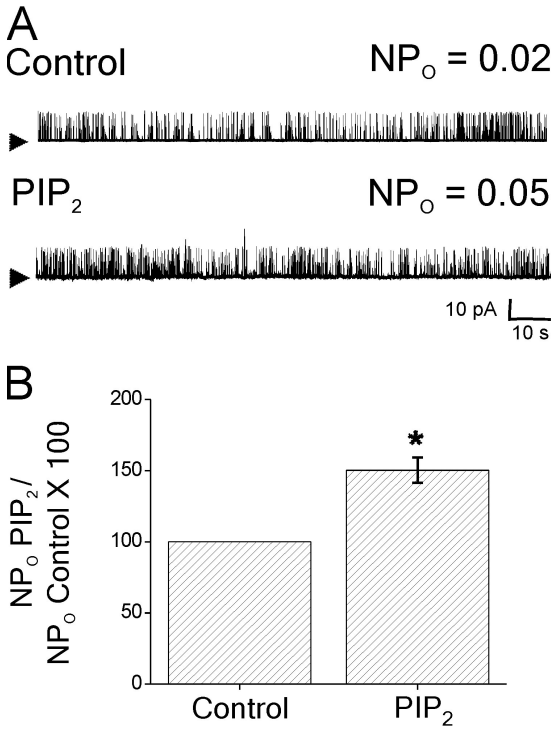

Figure 4. PIP_2 action on native BK channels in isolated skeletal muscle myocytes. (A) Unitary currents from an I/O patch obtained before (top) and after (bottom) a 5-min bath application of 10 μM PIP_2 show that the phosphoinositide causes an increase in BK NP_o that is markedly reduced when compared with that evoked by PIP_2 in vascular myocyte BK channels (Fig. 1, A and C). Arrowheads, baseline; upward deflections, channel openings. (B) Averaged PIP_2 responses of native skeletal muscle BK channels; *, $P < 0.05$; n = 4; V = 40 mV, Ca^{2+}_i = 10 μM.

activated cbv1 channels (Fig. 3 B), NP_o reaching 590 ± 15% of control. This indicates that cbv1 and its immediate lipid environment are sufficient for PIP_2 activation of BK channels. Having established that headgroup negative charge plays a critical role in this action, we probed whether positively charged residues in cbv1 could recognize the negatively charged PIP_2. Alanine substitution of positive residues clustered at the bottom of the pore-forming M2 domain of Kir6.2 channels attenuates PIP_2 modulation (Shyng et al., 2000). Similarly, positive residues clustered at the bottom of the pore-forming S6 segment of KCNQ1 are thought to contribute to PIP_2 action on KCNQ1/KCNE1 channels (Loussouarn et al., 2003). After identifying a cluster of positive residues in an equivalent region of cbv1, we probed PIP_2 in cbv1 where AAA substituted for RKK in the S6–S7 cytosolic linker (Fig. 3 A).

In I/O patches, RKKcbv1AAA currents were indistinguishable from those mediated by cbv1 (Fig. 3 C). In contrast to wt cbv1, PIP_2 applied to the cytosolic side of I/O patches expressing RKKcbv1AAA barely shifted the G/G_{max}–voltage curve (Fig. 3 C). PIP_2 differential action on wt cbv1 vs. RKKcbv1AAA was also evident from

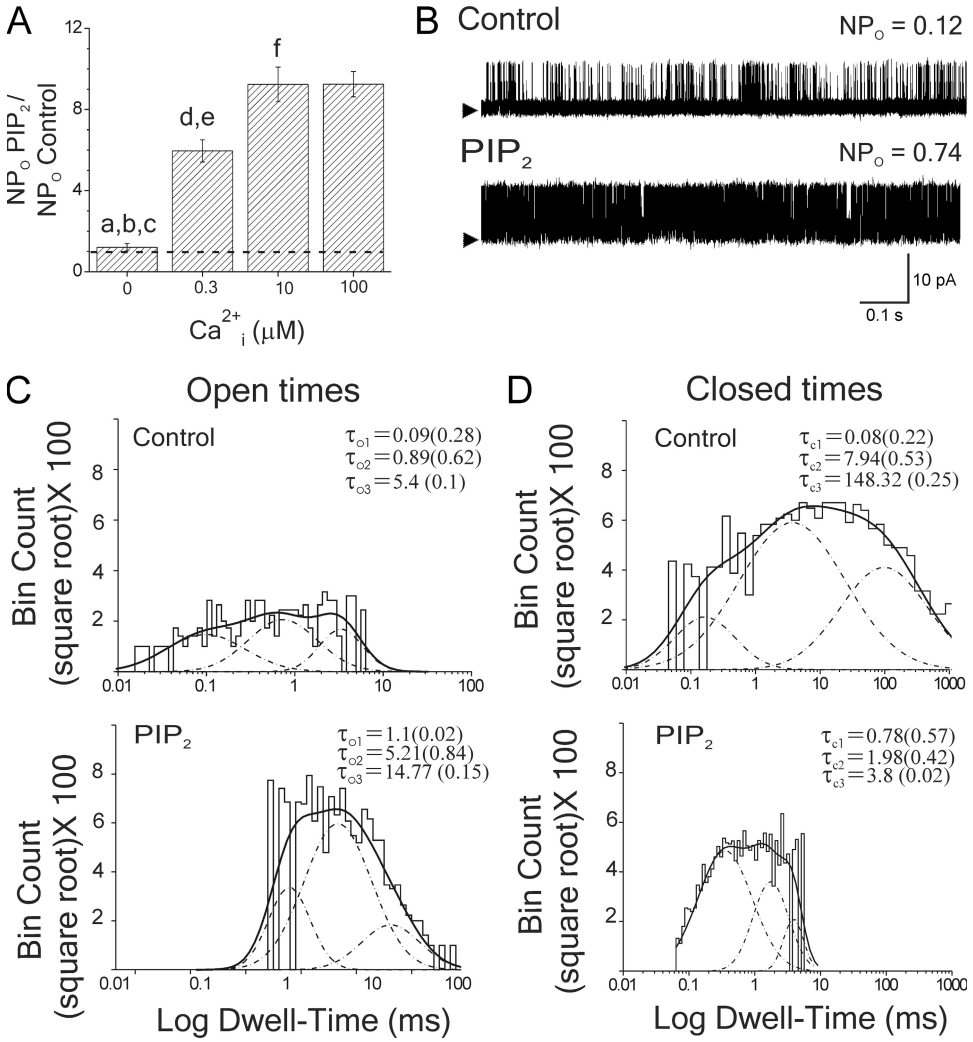

Figure 5. PIP_2 activates the BK channel by amplifying Ca^{2+}-driven gating, resulting in modifications of both open and closed times. (A) PIP_2 activation of cbv1 is negligible at zero nominal Ca^{2+}_i and reaches a maximum at 10 μM Ca^{2+}_i; (a) zero Ca^{2+}_i vs. 0.3 μM Ca^{2+}_i: $P < 0.001$; (b) zero Ca^{2+}_i vs. 10 μM Ca^{2+}_i: $P < 0.001$; (c) zero Ca^{2+}_i vs. 100 μM Ca^{2+}_i: $P < 0.001$; (d) 0.3 μM Ca^{2+}_i vs. 10 μM Ca^{2+}_i: $P < 0.001$; (e) 0.3 μM Ca^{2+}_i vs. 100 μM Ca^{2+}_i: $P < 0.001$; $n = 3$–12. (B) Single channel records in the absence (top) and presence (bottom) of 10 μM PIP_2 show that the lipid increases P_o from 0.06 to 0.43 (616% of control). Records were low-passed at 7 kHz and digitized at 35 kHz. Upward deflections: channel openings. (C) Open and (D) closed time distributions in control (top) and PIP_2 (bottom) from records shown in B. Each life time constant (τ) is shown in milliseconds, with its contribution to the total fit in parentheses. Each component of a fit is shown with a dotted line, and the composite fit is shown with a solid line; 40 mV; $Ca^{2+}_i = 0.3$ μM.

single-channel data: PIP_2 caused a mild increase in RKKcbv1AAA NP_o, which was drastically smaller than that in wt cbv1 (Fig. 3 D). Furthermore, exposing the mutant to increased PIP_2 (30 μM) raised NP_o to ~350% of control ($n = 4$), which is barely different from the response evoked by 10 μM PIP_2 in the mutant and significantly smaller than the response in wt cbv1. Therefore, the sequence RKK in the cbv1 S6–S7 linker is involved in PIP_2 activation of the BK channel.

To determine whether PIP_2 activation of cbv1 channels specifically depends on the S6–S7 RKK sequence or, rather, can also depend on positive amino acids located in other cbv1 cytosolic loops, we made the construct K239cbv1A. K239 is located in the S4–S5 cytosolic loop and is thus readily accessible to PIP_2 negative charges when the phosphoinositide is applied to the cytosolic membrane leaflet. After expression in *Xenopus laevis* oocytes, K239cbv1A rendered channel current events characteristic of BK (slo1) channels, such as high unitary conductance for K^+ (Fig. S1 A) and voltage dependence of channel gating (12.9 mV/e-fold change in channel activity) (Fig. 3 C). Under conditions identical to those used in the studies of PIP_2 action on wt cbv1 and RKKcbv1AAA channels, PIP_2 potentiated K239A-mediated current when studied at both macroscopic (Fig. 3 C) and single-channel levels (Fig. 3 D). Moreover, the magnitude of K239A channel activation in response to PIP_2 was identical to that observed with wt cbv1 (Fig. 3 D). Therefore, PIP_2 activation of cbv1 does not involve any positive amino acid residue that can be found in cbv1 cytosolic loops. Rather, the S6–S7 RKK and its flanking sequence, which meet criteria for a PIP_2 binding site (see Discussion), appear specifically involved. As found with PIP_2, PIP_3 action was also significantly blunted in RKKcbv1AAA, yet similar in wt cbv1 and the K239A mutant (Fig. S1), suggesting a common site(s) of action for PIP_2 and PIP_3.

Notably, PIP_2 action on cbv1 expressed in oocytes was significantly smaller than that observed with native channels in myocytes (Fig. 3 D vs. Fig. 2 D). Because cbv1+β_1 constitutes the cerebral artery myocyte BK, we next explored PIP_2 action on cbv1+β_1 expressed in

Xenopus oocytes. The presence of functional β_1 was confirmed by current characteristics, or a P_o increase with bath application of 10 μM 17β-estradiol to O/O patches (Bukiya et al., 2007). PIP_2 activation of cbv1 was consistently enhanced when β_1 was coexpressed (Fig. 3, E and F). Notably, the PIP_2 increase in cbv1+ β_1 NP_o (2,029 ± 286% of control) (Fig. 3 F) was similar to that in the myocyte native channel (Fig. 1 C). Thus, possible differences in the proteolipid environment around the BK channel complex between frog oocyte and rat myocyte membranes appear not to play a major role in PIP_2 action. Rather, the cbv1+ β_1 complex appears sufficient to support channel activation by PIP_2.

To determine whether the amplification of PIP_2 action is selective to the β subunit type that is predominant in smooth muscle (β_1), we tested PIP_2 action on cbv1+β_4 complexes. The presence of functional β_4 was confirmed by current characteristics, including refractoriness to iberiotoxin block (Bukiya et al., 2007). Under conditions identical to those used with cbv1+β_1, PIP_2 action on cbv1 was not amplified by β_4 (Fig. 3, E and F). Because the expression of a given β type shows high tissue specificity (Behrens et al., 2000; Brenner et al., 2000; Orio et al., 2002), the differential PIP_2 action on recombinant channels expressed in oocytes raised the speculation that drastic activation of native BK is restricted to cells expressing high amounts of β_1, such as vascular myocytes. Thus, we probed PIP_2 on native BK channels in another type of myocyte (the skeletal muscle fiber), where β_1 is barely expressed (Behrens et al., 2000; Brenner et al., 2000; Orio et al., 2002). Application of 10 μM PIP_2 to the cytosolic side of I/O patches from rat skeletal muscle fibers consistently caused channel activation (Fig. 4). However, this activation was drastically smaller than that evoked by PIP_2 in native vascular myocyte BK channels (Fig. 2 D, first column). Furthermore, PIP_2 action on native skeletal muscle native channels was indistinguishable from that observed with cbv1 in oocytes and significantly smaller than PIP_2 action on cbv1+β_1 channels (Fig. 3 F). Therefore, PIP_2 action is, indeed, strongest in tissues expressing BK channel complexes that contain β_1 subunits.

PIP_2 Modifies both Open and Closed Time Distributions

We next determined which PIP_2 actions lead to increased BK channel NP_o. A hallmark of BK channels is independent gating by voltage and Ca^{2+}_i. Application of PIP_2 to the cytosolic side of I/O patches expressing cbv1 resulted in a parallel leftward shift in the macroscopic current conductance (G/G_{max})–voltage curve (Fig. 3 C). Thus, the channel effective valence (z) obtained from these plots was identical in the absence and presence of PIP_2: $z = 1.71 \pm 0.03$ vs. 1.7 ± 0.04, $P > 0.5$ ($Ca^{2+}_i = 0.3$ μM). Therefore, the negatively charged lipid modifies P_o without affecting the effective gating charge.

A parallel leftward shift in the G/G_{max}–voltage relationship can be caused by an increase in the apparent

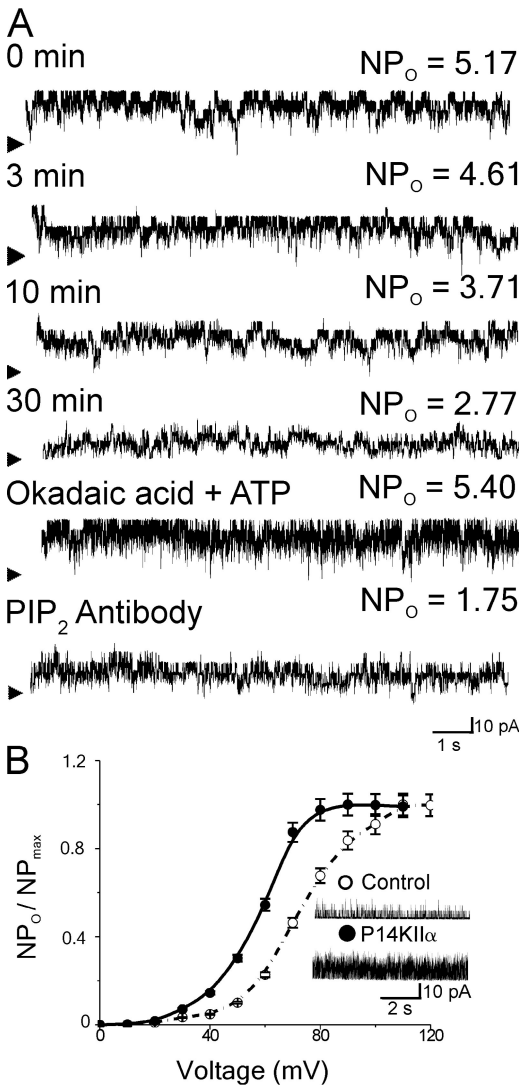

Figure 6. Endogenous PIP_2 maintains native BK channel activity. (A) Time course of vascular myocyte BK NP_o from an I/O patch. Intervals indicate time after patch excision. Arrowheads, baseline; upward deflections, channel openings. Bath application of 0.5 mM ATP and 0.1 μM okadaic acid (OA) increases NP_o ×5.4 times. Subsequent application of PIP_2 monoclonal antibodies (1:1,000) drastically reduces NP_o. V = 40 mV; Ca^{2+}_i = 3 μM. (B) Cotransfection of HEK cells with PI4KαII and cbv1+β_1 channel subunits causes a parallel leftward shift in the activation–voltage plot when compared with currents mediated by cbv1+β_1 alone; n = 5–7.

Ca^{2+} sensitivity of the channel (i.e., less Ca^{2+} is needed to obtain a given NP_o). To determine the Ca^{2+} dependence of PIP_2 action, we probed PIP_2 on cbv1 using solutions containing constant free Mg^{2+} (≈0.6 mM) and different, highly buffered Ca^{2+} levels. When the channel was primarily gated by voltage (i.e., zero nominal Ca^{2+}_i), PIP_2 barely modified NP_o (130% of control; Fig. 5 A). PIP_2-induced potentiation, however, was robust at 0.3 μM Ca^{2+}_i, reaching a maximum at 10 μM Ca^{2+}_i (Fig. 5 A), which suggests that PIP_2 increases NP_o by amplifying Ca^{2+}_i-driven gating.

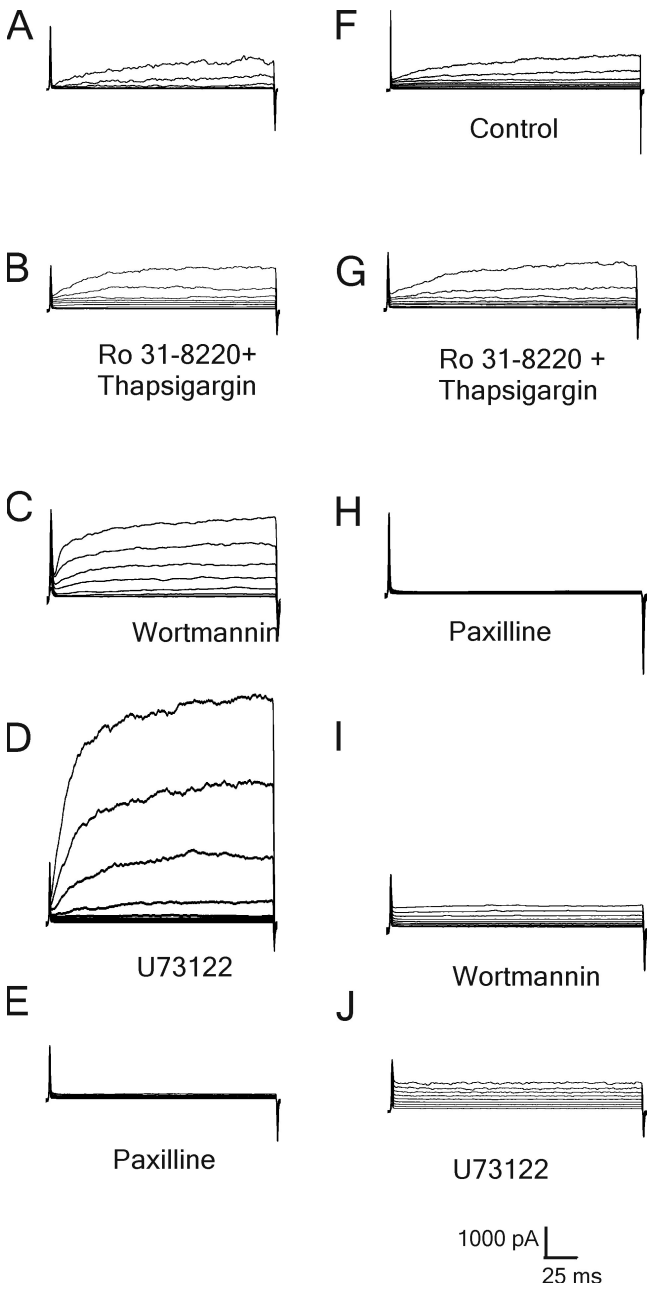

Figure 7. Endogenous PIP_2 activates native BK currents in the presence of blockers of PLC-mediated PIP_2 downstream products. Perforated patch recordings from two (A–E and F–J) freshly isolated cerebral artery myocytes bathed in physiological saline solution (PSS; composition in Materials and methods). Total outward K^+ currents were recorded in the continuous presence of 5 mM 4-AP and 0.1 mM niflumic acid. Bath application of 2 μM Ro31-8220 and 0.2 μM thapsigargin increases mean outward current by 95% (B vs. A, and G vs. F). Subsequent inhibition of PI3 kinase by 5 nM wortmannin further increases current by 184% from control (C). Inhibition of PLC by 25 μM U73122 drastically increases current (D), likely due to buildup of PIP_2 in the membrane. The current is blocked by 0.3 μM paxilline (E and H), indicating it is mediated by BK channels. Preapplication of paxilline, a selective BK channel blocker, prevents both wortmannin (I) and U73122 (J) actions ($n = 5$–6).

Data from patches containing one functional channel revealed that PIP_2 increase in P_o (Fig. 5 B) was similar to the potentiation of NP_o (Fig. 3 D). Therefore, it appears that PIP_2 action on NP_o, and thus current, is due solely to modification of P_o. The increase in P_o evoked by PIP_2 was always associated with a robust increase in the frequency of channel bursts (Fig. 5 B). However, the PIP_2 effect on P_o results from several PIP_2 actions, as revealed by dwell-time distribution analysis. PIP_2 caused a major shift in the open channel population toward longer openings, which resulted in an ~500% increase in channel mean open time (Fig. 5 C). In addition, PIP_2 drastically reduced the duration of the channel long closures, which resulted in increased channel bursting (Fig. 5 B) and a drastic reduction in the channel mean closed time, the latter reaching 3.3% of control (Fig. 5 D). In brief, PIP_2 increases BK P_o by both stabilization of channel openings and destabilization of channel long closures.

Regulation of BK Channels by Endogenous PIP_2

After showing that exogenously applied PIP_2 enhances BK P_o, we next determined whether channel activity could be modulated by endogenous PIP_2. As reported with BK channels from sheep basilar artery myocytes (Lin et al., 2003), cerebrovascular BK channel NP_o continuously ran down after patch excision, reaching ~62% of control after 30 min (Fig. 6 A). BK NP_o is modulated by protein phosphatases and kinases that remain associated with the excised patch (Lin et al., 2003). Additionally, activation of lipid kinases via Mg-ATP increases membrane PIP_2 levels and thus modulates BK channel activity (Huang et al., 1998). To begin to test whether endogenous PIP_2 contributes to regulating BK NP_o, we evaluated a possible reversion of NP_o rundown in the excised patch by lipid kinase activation.

In the presence of phosphatase inhibition (0.1 μM okadaic acid; Lin et al., 2003), bath application of Mg-ATP (0.5 mM) totally rescued the channel rundown (Fig. 6 A, fifth row), which likely reflects channel activation by PIP_2 that is being regenerated via PI4KIIα (Yaradanakul et al., 2007). Moreover, PIP_2 antibodies (monoclonal 1:1,000) applied on top of Mg-ATP to the cytosolic side of the plasma membrane dropped NP_o to <35% of control, strongly suggesting the involvement of endogenous PIP_2 in controlling BK channel activity in the native membrane. Finally, cotransfection of HEK293 cells with cbv1+β_1 channels and PI4kinaseIIα resulted in robust potentiation of NP_o (Fig. 6 B). Because transfection of PI4KIIα leads to increased PIP_2 levels (Yaradanakul et al., 2007), the result supports the notion that augmentation in membrane PIP_2 levels leads to increased cbv1+β_1 NP_o.

The possibility of a modulatory role of endogenous PIP_2 on BK channels was also tested by using pharmacological manipulations of macroscopic current in intact,

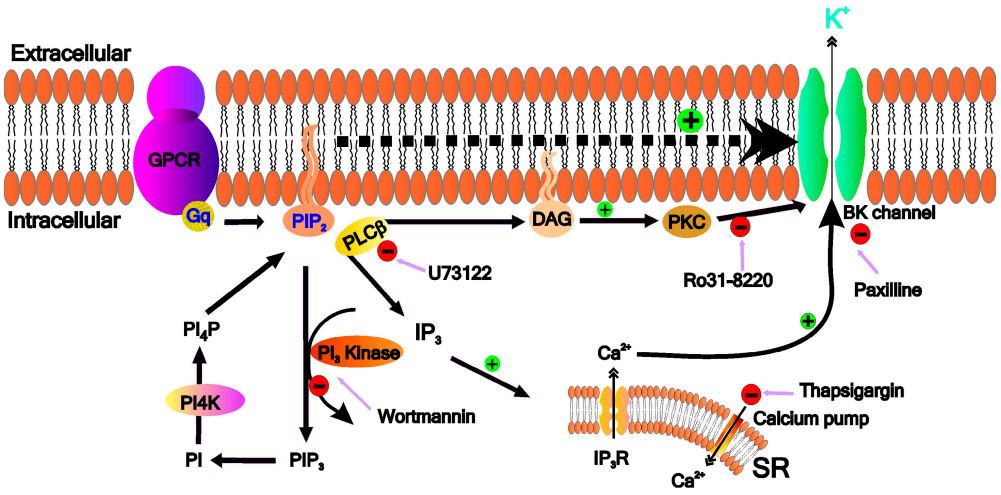

Figure 8. Indirect (classical) and direct (novel) mechanisms of PIP_2 action on BK currents. Activated PLC via Gq, determined by either ligand binding to a Gq-coupled receptor (GPCR) or constitutive activity, cleaves PIP_2 into PIP_3, IP3, and DAG. IP3 releases Ca^{2+} from the sarcoplasmic reticulum (SR), raising Ca^{2+}_i, whereas DAG activates PKC in the presence of Ca^{2+}. BK channel modulation by PKC and Ca^{2+}_i controls the degree of vascular myocyte contraction. Therefore, by generating DAG and IP3, PIP_2 indirectly modulates BK channels and, thus, vascular tone. We demonstrate that PIP_2 itself and other membrane phosphoinositides directly activate BK channels, that is, in the absence of cell integrity or organelles or in the continuous presence of cytosolic messengers. This activation involves the negative charges of the phosphoinositide headgroup and the sequence of positive residues RKK in the cbv1 S6–S7 cytosolic linker. However, PIP_2 activation is drastically and distinctly amplified by the channel accessory subunit of the β_1 type, which is abundantly expressed in smooth muscle. In intact myocytes, inhibition of PLC by U73122 increases paxilline-sensitive BK currents in the presence of a PI3 kinase blocker (wortmannin), PKC inhibitor (Ro 31-8220), and a selective blocker of the sarcoplasmic reticulum Ca^{2+}-ATPase (thapsigargin). Under these conditions, PLC inhibition increases membrane PIP_2 (Narayanan et al., 1994), which leads to increased BK current in the intact cell (see main text).

freshly isolated myocytes. We used perforated patches to keep the intracellular milieu intact and recorded total outward currents in PSS containing 0.1 mM niflumic acid to block Ca^{2+}-activated Cl^- channels (Ledoux et al., 2005) and 5 mM 4-aminopyridine to block voltage-gated K^+ channels other than BK (Thebaud et al., 2004). Under these conditions, myocytes displayed noninactivating outward currents (e.g., 483 pA peak amplitude at 100 mV; Fig. 7, A and F), their major component reported to be the BK current (Catacuzzeno et al., 2000).

Inhibition of PKC (2 μM Ro31-8220; Barman et al., 2004) combined with a block of SR Ca^{2+}-ATPase (0.2 μM thapsigargin; Goforth et al., 2002) caused a mild but consistent increase in current (Fig. 7, B and G), suggesting that PKC inhibition of myocyte BK channels (Barman et al., 2004) prevails over channel activation by sarcoplasmic Ca^{2+} (Goforth et al., 2002) (Fig. 8). To build up membrane PIP_2, we inhibited PLC (25 μM U73122; Wilkerson et al., 2006), the major PIP_2-metabolizing enzyme (Tolloczko et al., 2002). This treatment, however, can reroute PIP_2 toward formation of PI3kinase-mediated PIP_3 (Fruman et al., 1998; Suh et al., 2006), a powerful BK channel activator (Fig. 2). Thus, we first blocked PI3kinase (5 nM wortmannin; Arcaro and Wymann, 1993), which mildly increased current, likely due to PIP_2–PIP_3 buildup (Fruman et al., 1998; Suh et al., 2006). Subsequent PLC inhibition caused a dramatic increase in both activation slope and amplitude of current (Fig. 7 D), with peak amplitude reaching 6,608.5 ± 1,983.1% of control (n = 4). The result indicates that PLC tonically controls the noninactivating K^+ current in intact cerebral artery myocytes. These currents were totally suppressed by 0.3 μM paxilline (Fig. 7 E) or 0.1 μM iberiotoxin (not depicted), identifying the PLC-regulated current as of the BK type (Weiger et al., 2002).

Under block of PKC and SR Ca^{2+}-ATPase (final targets of IP3 and DAG; Fig. 8), the potentiation of current that results from PLC inhibition could be attributed to (a) buildup of PIP_2 and related phosphoinositide or (b) depletion of IP3 and DAG with loss of a putative direct inhibition of the channel caused by one or both metabolites. IP3, however, potentiates myocyte BK channels (Cai et al., 2005). On the other hand, 2 μM DOG (a cell-permeable DAG analogue) applied to the cytosolic side of I/O patches excised from cerebral artery myocytes evoked no major effect on BK channel activity, with NP_o in DOG reaching 78.4 ± 2.4% of controls (n = 4). Therefore, the dramatic increase in BK current caused by PLC inhibition in addition to the PI3kinase block has to be primarily attributed to a direct PIP_2 activation of BK channels. Consistent with this interpretation, preincubation with paxilline precluded PI3kinase and/or PLC inhibition from affecting current (Fig. 7, I and J). Collectively, the results in freshly isolated cerebral artery myocytes reinforce the idea that endogenous PIP_2 controls BK currents in the myocyte membrane.

PIP_2 Regulates Cerebrovascular Tone via BK Channels

We next determined any possible contribution of PIP_2 direct modulation of myocyte BK currents to modifications in vascular tone using endothelium-free, pressurized

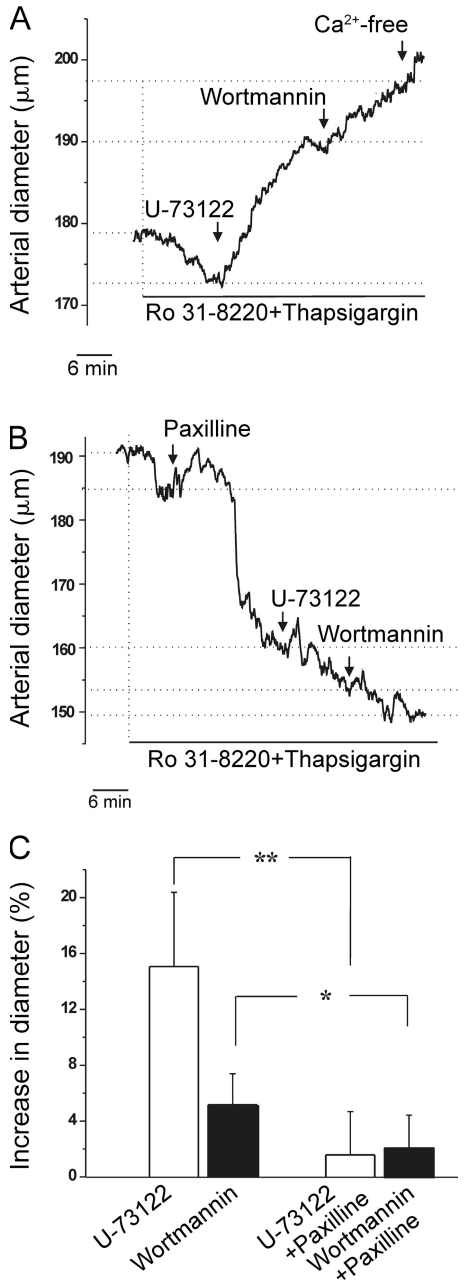

Figure 9. Endogenous PIP_2 dilates cerebral arteries via BK channels. Diameter traces from de-endothelized arteries after developing myogenic tone. (A) In the presence of 2 μM Ro 31-8220 and 0.2 μM thapsigargin, PLC inhibition (25 μM U73122) causes a robust dilation (+15.1%), which is further increased by 5 nM wortmannin. Maximal dilation is evoked by Ca^{2+}-free solution. (B) BK channel block (0.3 μM paxilline) reduces diameter (−13%) and almost totally blunts U73122 and wortmannin actions. In A and B, a vertical line indicates the time at which Ro 31-8220 and thapsigargin were applied; horizontal lines help to visualize diameter changes. (C) Averaged diameters; **, $P < 0.01$; *, $P < 0.05$; $n = 4$.

cerebral arteries that spontaneously develop myogenic tone (Liu et al., 2004). After myogenic tone developed, arterial diameter reached 186.9 ± 7.1 μm ($n = 6$), with maximal contraction and dilation being obtained by perfusing the vessel with 60 mM KCl at the beginning, and Ca^{2+}-free solution at the end of each experiment, respectively (Fig. 9 A). Under block of PKC and SR Ca^{2+}-ATPase, PLC inhibition, which increased BK current (Fig. 7), increased diameter (+15.1 ± 0.1%; $n = 3$) (Fig. 9 A). Subsequent PI3 kinase inhibition caused an additional, mild dilation (+5.2 ± 2.2%; $n = 3$), consistent with the mild increase in BK current caused by this treatment (Fig. 7). Data strongly suggest that PIP_2 and/or other membrane phosphoinositides directly modulate myogenic tone of cerebral arteries. In the presence of paxilline, a selective BK channel blocker, neither PLC inhibition nor PI3 kinase block caused major dilation: 5.5 ± 4.4% ($n = 4$) and 6.4 ± 4.3% (Fig. 9 B), indicating that the phosphoinositide effect on myogenic tone is primarily mediated via BK channels.

DISCUSSION

Our study identifies a new mechanism by which membrane PIP_2 controls smooth muscle BK currents and, thus, vascular tone: an increase in channel steady-state activity due to an apparent direct interaction between PIP_2 and the BK protein complex. Thus, PIP_2 controls BK currents in cerebral artery myocytes via two mechanisms (Fig. 8): (1) indirect, which involves the well-known PLC signaling pathway, and (2) direct, through amplification of Ca^{2+}-driven gating of the BK channel with consequent increase in P_o. This amplification is secondary to recognition of negative charge and the inositol moiety in the PIP_2 headgroup by the BK channel α subunit, with drastic potentiation by the smooth muscle-abundant accessory β_1 subunit.

PIP_2 Direct Mechanism: Molecular Players

Most biological actions of PIP_2 that occur through binding to specific protein sites require electrostatic interactions between negative charges in the PIP_2 headgroup and positive charges in the target site. This has been demonstrated for PIP_2 direct regulation of several types of ion channels (Fan and Makielski, 1997; Shyng et al., 2000; Suh and Hille, 2005; Rohács, 2007; Voets and Nilius, 2007). The critical dependence of BK channel activation on phosphoinositide's negative charges demonstrated here supports the hypothesis of a protein recognition site being involved. In addition, data show that PI5P is more effective than 1,2-dipalmitoyl-L-α-phosphatidyl-D-myo-inositol 4-monophosphate (PI4P) in increasing BK NP_o (unpublished data). This PIP isomer specificity also implicates a defined protein site in PIP_2 action. While PIP_2 activation of BK is drastically amplified by β_1 (Fig. 3, E and F), it is evident in homomeric cbv1 channels (Fig. 3, B and F). This result indicates that cbv1 is sufficient to respond to PIP_2 and suggests that the subunit contains a PIP_2 binding site(s).

PIP_2 interacts with Kir channels at several intracellular sites, most of which have positively charged residues (Shyng et al., 2000; Suh and Hille, 2005). Similarly, positive residues at the end of S6 are thought to contribute to the PIP_2 sensitivity of KCNQ1/KCNE1 channels (Loussouarn et al., 2003). Positive residues at an equivalent location in TRP channels are also proposed for recognition of PIP_2 (Rohács, 2007). It is noteworthy that Ala substitutions of RKK in the equivalent region of cbv1 drastically decreased PIP_2 action (Fig. 3 D) without modifying basic current phenotype (Fig. 3 C). Thus, the reduced PIP_2 action in the mutant is not due to an overall change in cbv1 protein conformation caused by the mutation. Rather, neutralization of RKK specifically prevents cbv1 from effectively sensing PIP_2. Collectively, our data suggest that PIP_2 directly interacts with cbv1 at an RKK cluster via electrostatic interactions to activate BK channels. In the absence of crystallographic data of BK channels, it is not possible to determine whether the RKK cluster is an actual PIP_2 binding site or a transducing region that connects the channel gate with a PIP_2 binding site(s) located elsewhere in the cbv1 (α) subunit. From 25 crystallographic structures of proteins that bind PIP_2, however, several major criteria for a PIP_2 binding site emerge: (1) it must contain at least two positively charged residues (Arg and Lys); (2) among these, at least one should be Arg; (3) the presence of at least one hydrophobic residue nearby; (4) involvement of at least five interacting residues (Rosenhouse-Dantsker and Logothetis, 2007). Remarkably, the RKK and its nearby context in cbv1 (Fig. 3 A) fulfill three out of these four criteria. While we did not test the fourth criterion, we note that the RKKcbv1AAA mutant is not completely insensitive to PIP_2 (Fig. 4 D), suggesting that residues other than the RKK triplet also play a role in PIP_2 sensing. Interestingly, cbv1 contains a large intracellular structure with 110 positive residues, many of which are potentially able to interact with membrane PIP_2. Future studies using alanine scanning mutagenesis will help to clarify whether one or more of these residues are involved in PIP_2 regulation of BK channel activity.

A variety of BK α subunit isoforms resulting from alternative splicing of Slo1 have been identified in different tissues and species (Xie and McCobb, 1998; Salkoff et al., 2006), and their PIP_2 sensitivity remains to be determined. Following expression in *X.* oocytes, bslo (from bovine aorta) channel activity is significantly increased by acute exposure to brain phosphoinositides (Liu et al., 2003). Notably, bslo subunits also contain the RKK sequence in their S6–S7 cytosolic loop.

In contrast to Slo1, BK β_1 subunit cytosolic regions do not include RKK sequences. However, BK β_1 cytosolic C and N ends both contain scattered, positively charged residues that are absent in BK β_4 subunits (Behrens et al., 2000; Brenner et al., 2000). Thus, we cannot currently rule out that PIP_2 occupation of additional binding sites located in BK β_1 accessory subunits contributes to amplification of PIP_2 action on cbv1 activity by β_1 subunits. On the other hand, β_1 subunit-induced enhancement of the BK channel's apparent calcium sensitivity has been primarily attributed to changes in voltage-dependent gating of Slo1 (Bao and Cox, 2005), which occur with reduction in both gating charge and channel intrinsic open-to-closed equilibrium, and enhanced coupling between voltage sensing and channel opening (Orio and Latorre, 2005; Wang and Brenner, 2006). Disregarding the mechanistic underpinnings, amplification of PIP_2 action on cbv1 activity by BK β_1 subunits appears to indicate that conformational changes in cbv1 that occur upon PIP_2 interaction with RKK in the channel S6–S7 cytosolic loop are functionally coupled to the channel voltage sensor movements.

PIP_2 Direct Activation of BK Channels Differs from that Caused by Other Negatively Charged Lipids

BK channel steady-state activity is regulated by negatively charged lipids other than PIP_2, the best studied group being fatty acids (FA). FA direct activation of BK channels, however, differs from PIP_2-induced activation in several critical aspects. First, FAs increase P_o without a major effect, if any, on channel mean open time (Clarke et al., 2002). In contrast, PIP_2 drastically enhances mean open time by stabilizing medium and long channel openings (Fig. 5 C). Second, palmitoylcoenzyme-A (that is, "a membrane-impermeable fatty acid") is effective only when applied to the extracellular membrane leaflet (Clarke et al., 2003). PIP_2, however, activates BK channels by accessing the channel via its intracellular side (Fig. 1 C), which likely allows phosphoinositide sensing by the RKK cluster of positive residues in the cytosolic S6–S7 linker of the channel (Fig. 3, A–D). Third, FA action appears Ca^{2+}_i independent (Clarke et al., 2002). In contrast, PIP_2 increases activity through amplification of Ca^{2+}_i-driven gating. This mechanism is supported by the following observations: (a) PIP_2 action in solutions having zero nominal Ca^{2+}_i plus 5 mM EGTA to chelate trace amounts of the metal is negligible (Fig. 3 A); (b) PIP_2 action is blunted by shielding negative charge with 300 mM Na^+ in the bath solution (Vaithianathan, T., P. Liu, and A. Dopico. 2006. *Society for Neuroscience, Online.* 627.5); (c) PIP_2 causes a parallel shift in the G/Gmax–voltage plot (Fig. 3 C); and (d) PIP_2 action is potentiated by β_1, but not β_4, subunits. Interestingly, PIP_2 readily and consistently activates BK channels only if applied to the cytosolic side of the channel, where the Ca^{2+} sensors are located (Cai et al., 2005).

Finally, BK channel activation by arachidonic acid and analogues has recently been linked to the ability of these FAs to remove β_2- or β_3-mediated BK inactivation. Thus, these FAs fail to modulate slo1 channel function (Sun et al., 2007). In contrast, we demonstrate that (a) the BK channel-forming subunit is sufficient for PIP_2 action; (b) this action is amplified by β_1 subunits, which do not

introduce channel inactivation (Meera et al., 1996; Brenner et al., 2000), and (c) PIP_2 action is poor on native skeletal muscle BK channels (Fig. 4) where β_3 subunits are significantly expressed (Behrens et al., 2000).

As found here with PIP_2, lithocholate and other structurally related cholane derivatives directly increase BK NP_o by modifying both open and closed time distributions (Bukiya et al., 2007). Differing from PIP_2 action, however, lithocholate fails to activate cbv1 channels even at concentrations that are maximally effective on native BK or cbv1+β_1 channels; the presence of the β_1 subunit is required for lithocholate to activate BK channels (Bukiya et al., 2007). In conclusion, PIP_2 direct activation of BK channels shows unique structural and functional features when compared with the direct activation of these channels by other negatively charged lipids.

Pathophysiological Implications

Our study demonstrates for the first time that BK channels belong to the group of ion channels that PIP_2 directly regulates (Hilgemann and Ball, 1996; Fan and Makielski, 1997; Runnels et al., 2002; Rohács et al., 2003; Chemin et al., 2005; Suh and Hille, 2005; Brauchi et al., 2007; Hilgemann, 2007; Rohács 2007; Voets and Nilius, 2007). An important addition to current knowledge on PIP_2 regulation of ion channels is that the final PIP_2 effect is critically determined by channel accessory subunits, and such a mechanism can be subunit specific. Moreover, the differential expression of BK accessory subunits across tissues (Behrens et al., 2000; Brenner et al., 2000; Orio et al., 2002) raises the possibility that a direct PIP_2 modulation of BK channel function is specifically relevant in tissues where the β_1 subunit is highly expressed. Indeed, while PIP_2 robustly activates native BK channels in vascular smooth muscle (Fig. 1), where β_1 subunits are highly expressed, it mildly activates native BK channels in skeletal muscle, where β_1 subunits are barely detected (Behrens et al., 2000).

In conclusion, we demonstrate a new mechanism for modulating BK currents in cerebrovascular smooth muscle: PIP_2 direct modulation of BK channel gating. Our data, obtained with recombinant proteins, cells, and intact arteries from the cerebrovascular system, opens the possibility of determining the role of the direct interaction between PIP_2 and BK channels in pathophysiological processes leading to disease, such as cerebrovascular spasm and ischemic stroke. Moreover, determining the structural requirements in PIP_2 and the BK complex for modulating channel function may pave the way for designing new agents to control myogenic tone.

The authors thank Donald Hilgemann for helpful criticism and David Armbruster for critically reading the manuscript.

This work was supported by grants AA11560 and HL77424 (A. Dopico), GM-61943 and HL-58133 (Z. Fan), and AHA SouthEast Postdoctoral Fellowships (J. Liu, P. Liu).

David C. Gadsby served as editor.

Submitted: 23 October 2007
Accepted: 29 May 2008

REFERENCES

Arcaro, A., and M.P. Wymann. 1993. Wortmannin is a potent phosphatidylinositol 3-kinase inhibitor: the role of phosphatidylinositol 3,4,5-trisphosphate in neutrophil responses. *Biochem. J.* 296:297–301.

Bao, L., and D.H. Cox. 2005. Gating and ionic currents reveal how the BKCa channel's Ca^{2+} sensitivity is enhanced by its β1 subunit. *J. Gen. Physiol.* 126:393–412.

Barman, S., S. Zhu, and R. White. 2004. PKC activates BKCa channels in rat pulmonary arterial smooth muscle via cGMP-dependent protein kinase. *Am. J. Physiol. Lung Cell Mol. Physiol.* 286:L149–L155.

Behrens, R., A. Nolting, F. Reimann, M. Schwarz, R. Waldschutz, and O. Pongs. 2000. hKCNMB3 and hKCNMB4, cloning and characterization of two members of the large-conductance calcium-activated potassium channel β subunit family. *FEBS Lett.* 474:99–106.

Brauchi, S., G. Orta, C. Mascayano, M. Salazar, N. Raddatz, H. Urbina, E. Rosenmann, F. Gonzalez-Nilo, and R. Latorre. 2007. Dissection of the components for PIP_2 activation and thermosensation in TRP channels. *Proc. Natl. Acad. Sci. USA.* 104:10246–10251.

Brayden, J.E., and M. Nelson. 1992. Regulation of arterial tone by activation of calcium-dependent potassium channels. *Science.* 256:532–535.

Brenner, R., T.J. Jegla, A. Wickenden, Y. Liu, and R.W. Aldrich. 2000. Cloning and functional characterization of novel large conductance calcium-activated potassium channel β subunits, hKCNMB3 and hKCNMB4. *J. Biol. Chem.* 275:6453–6461.

Bukiya, A.N., J. Liu, L. Toro, and A. Dopico. 2007. β1 (KCNMB1) subunits mediate lithocholate activation of large-conductance Ca^{2+}-activated K^+ channels and dilation in small, resistance-size arteries. *Mol. Pharmacol.* 72:359–369.

Cai, F., X. Zeng, Y. Yang, Z. Liu, M. Li, W. Zhou, and J. Pei. 2005. Effect of IP3 on BK channels of porcine coronary artery smooth muscle cells. *Sheng Li Xue Bao.* 57:303–309.

Catacuzzeno, L., D. Pisconti, A. Harper, A. Petris, and F. Franciolini. 2000. Characterization of the large-conductance Ca-activated K channel in myocytes of rat saphenous artery. *Pflugers Arch.* 441:208–218.

Chemin, J., A. Patel, F. Duprat, I. Lauritzen, M. Lazdunski, and E. Honore. 2005. A phospholipid sensor controls mechanogating of the K^+ channel TREK-1. *EMBO J.* 24:44–53.

Cho, H., Y.A. Kim, and W.K. Ho. 2006. Phosphate number and acyl chain length determine the subcellular location and lateral mobility of phosphoinositides. *Mol. Cells.* 22:97–103.

Clarke, A.L., S. Petrou, J. Jr. Walsh, and J. Singer. 2002. Modulation of BK(Ca) channel activity by fatty acids: structural requirements and mechanism of action. *Am. J. Physiol. Cell Physiol.* 283:C1441–C1453.

Clarke, A.L., S. Petrou, J. Jr. Walsh, and J. Singer. 2003. Site of action of fatty acids and other charged lipids on BKCa channels from arterial smooth muscle cells. *Am. J. Physiol. Cell Physiol.* 284:C607–C619.

Crowley, J.J., S.N. Treistman, and A.M. Dopico. 2003. Cholesterol antagonizes ethanol potentiation of human brain BKCa channels reconstituted into phospholipid bilayers. *Mol. Pharmacol.* 64:365–372.

Dopico, A.M. 2003. Ethanol sensitivity of BK (Ca) channels from arterial smooth muscle does not require the presence of the β1-subunit. *Am. J. Physiol. Cell Physiol.* 284:C1468–C1480.

Dopico, A.M., V. Anantharam, and S. Treistman. 1998. Ethanol increases the activity of Ca^{2+}-dependent K^+ (mslo) channels: functional interaction with cytosolic Ca^{2+}. *J. Pharmacol. Exp. Ther.* 284:258–268.

Fan, Z., and J.C. Makielski. 1997. Anionic phospholipids activate ATP-sensitive potassium channels. *J. Biol. Chem.* 272(9):5388–5395.

Faraci, F.M., and D. Heistad. 1998. Regulation of the cerebral circulation: role of endothelium and potassium channels. *Physiol. Rev.* 78:53–97.

Fenwick, E.M., A. Marty, and E. Neher. 1982. Sodium and calcium channels in bovine chromaffin cells. *J. Physiol.* 331:599–635.

Flanagan, L.A., C.C. Cunningham, J. Chen, G.D. Prestwich, K.S. Kosik, and P.A. Janmey. 1997. The structure of divalent cation-induced aggregates of PIP_2 and their alteration by gelsolin and tau. *Biophys. J.* 73:1440–1447.

Fruman, D.A., R. Meyers, and L. Cantley. 1998. Phosphoinositide kinases. *Annu. Rev. Biochem.* 67:481–507.

Goforth, P.B., R. Bertram, F. Khan, M. Zhang, A. Sherman, and L. Satin. 2002. Calcium-activated K^+ channels of mouse β cells are controlled by both store and cytoplasmic Ca^{2+}: experimental and theoretical studies. *J. Gen. Physiol.* 120:307–322.

Hilgemann, D. 2007. On the physiological roles of PIP(2) at cardiac Na^+ Ca^{2+} exchangers and K(ATP) channels: a long journey from membrane biophysics into cell biology. *J. Physiol.* 582:903–909.

Hilgemann, D., and R. Ball. 1996. Regulation of cardiac Na^+,Ca^{2+} exchange and KATP potassium channels by PIP_2. *Science.* 273:956–959.

Huang, C.L., S. Feng, and D. Hilgemann. 1998. Direct activation of inward rectifier potassium channels by PIP_2 and its stabilization by Gβγ. *Nature.* 391:803–806.

Jaggar, J.H. 2001. Intravascular pressure regulates local and global Ca^{2+} signaling in cerebral artery smooth muscle cells. *Am. J. Physiol. Cell Physiol.* 281:C439–C448.

Jaggar, J., A. Li, H. Parfenova, J. Liu, E. Umstot, A. Dopico, and C. Leffler. 2005. Heme is a carbon monoxide receptor for large-conductance Ca^{2+}-activated K^+ channels. *Circ. Res.* 97:805–812.

Jaggar, J., G. Wellman, T. Heppner, V. Porter, G. Perez, M. Gollasch, T. Kleppisch, M. Rubart, A. Stevenson, W. Lederer, et al. 1998. Ca^{2+} channels, ryanodine receptors and Ca^{2+}-activated K^+ channels: a functional unit for regulating arterial tone. *Acta Physiol. Scand.* 164:577–587.

Knot, H.J., and M.T. Nelson. 1998. Regulation of arterial diameter and wall [Ca^{2+}] in cerebral arteries of rat by membrane potential and intravascular pressure. *J. Physiol.* 508:199–209.

Laux, T., K. Fukami, M. Thelen, T. Golub, D. Frey, and P. Caroni. 2000. GAP43, MARCKS, and CAP23 modulate PI(4,5)P(2) at plasmalemmal rafts, and regulate cell cortex actin dynamics through a common mechanism. *J. Cell Biol.* 149:1455–1472.

Ledoux, J., I. Greenwood, and N. Leblanc. 2005. Dynamics of Ca^{2+}-dependent Cl^- channel modulation by niflumic acid in rabbit coronary arterial myocytes. *Mol. Pharmacol.* 67:163–173.

Lin, M.T., D. Hessinger, W. Pearce, and L. Longo. 2003. Developmental differences in Ca^{2+}-activated K^+ channel activity in ovine basilar artery. *Am. J. Physiol. Heart Circ. Physiol.* 285:H701–H709.

Lin, M.T., L.D. Longo, W.J. Pearce, and D.A. Hessinger. 2005. Ca^{2+}-activated K^+ channel-associated phosphatase and kinase activities during development. *Am. J. Physiol. Heart Circ. Physiol.* 289:H414–H425.

Liu, P., L. Gao, M. Asuncion-Chin, Z. Fan, and A. Dopico. 2003. Phosphoinositides increase Bslo channel activity. *Biophys. J.* 84:2654.

Liu, P., A. Ahmed, J. Jaggar, and A. Dopico. 2004. Essential role for smooth muscle BK channels in alcohol-induced cerebrovascular constriction. *Proc. Natl. Acad. Sci. USA.* 101:18217–18222.

Loussouarn, G., K. Park, C. Bellocq, I. Baro, F. Charpentier, and D. Escande. 2003. Phosphatidylinositol-4,5-bisphosphate, PIP2, controls KCNQ1/KCNE1 voltage-gated potassium channels: a functional homology between voltage-gated and inward rectifier K^+ channels. *EMBO J.* 22:5412–5421.

McKillen, H.C., N.W. Davies, P.R. Stanfield, and N.B. Standen. 1994. The effect of intracellular anions on ATP-dependent potassium channels of rat skeletal muscle. *J. Physiol.* 479:341–351.

McLaughlin, S., and D. Murray. 2005. Plasma membrane phosphoinositide organization by protein electrostatics. *Nature.* 438:605–611.

Meera, P., M. Wallner, Z. Jiang, and L. Toro. 1996. A calcium switch for the functional coupling between α (hslo) and β subunits (KV,Ca β) of maxi K channels. *FEBS Lett.* 382:84–88.

Meininger, G.A., and M. Davis. 1992. Cellular mechanisms involved in the vascular myogenic response. *Am. J. Physiol.* 263:H647–H659.

Nahorski, S.R., R. Wilcox, J. Mackrill, and R. Challiss. 1994. Phosphoinositide-derived second messengers and the regulation of Ca^{2+} in vascular smooth muscle. *J. Hypertens. Suppl.* 12:S133–S143.

Narayanan, J., M. Imig, R.J. Roman, and D.R. Harder. 1994. Pressurization of isolated renal arteries increases inositol trisphosphate and diacylglycerol. *Am. J. Physiol.* 266:H1840–H1845.

Orio, P., and R. Latorre. 2005. Differential effects of β1 and β2 subunits on BK channel activity. *J. Gen. Physiol.* 125:395–411.

Orio, P., P. Rojas, G. Ferreira, and R. Latorre. 2002. New disguises for an old channel: MaxiK channel β subunits. *News. Physiol. Sci.* 17:156–161.

Park, J.B., H. Kim, P. Ryu, and E. Moczydlowski. 2003. Effect of phosphatidylserine on unitary conductance and Ba^{2+} block of the BK Ca^{2+}-activated K^+ channel: re-examination of the surface charge hypothesis. *J. Gen. Physiol.* 121:375–397.

Pérez, G.J., A. Bonev, and M. Nelson. 2001. Micromolar Ca^{2+} from sparks activates Ca^{2+}-sensitive K^+ channels in rat cerebral artery smooth muscle. *Am. J. Physiol.* 281:C1769–C1775.

Quinn, K.V., Y. Cui, J. Giblin, L. Clapp, and A. Tinker. 2003. Do anionic phospholipids serve as cofactors or second messengers for the regulation of activity of cloned ATP-sensitive K^+ channels? *Circ. Res.* 93:646–655.

Rohács, T. 2007. Regulation of transient receptor potential (TRP) channels by phosphoinositides. *Pflugers Arch.* 453:753–762.

Rohács, T., C. Lopes, T. Jin, P. Ramdya, Z. Molnar, and D. Logothetis. 2003. Specificity of activation by phosphoinositides determines lipid regulation of Kir channels. *Proc. Natl. Acad. Sci. USA.* 100:745–750.

Rohács, T., J. Chen, G.D. Prestwich, and D.E. Logothetis. 1999. Distinct specificities of inwardly rectifying K^+ channels for phosphoinositides. *J. Biol. Chem.* 274:36065–36072.

Rosenhouse-Dantsker, A., and D.E. Logothetis. 2007. Molecular characteristics of phosphoinositide binding. *Pflugers Arch.* 455:291–296.

Runnels, L.W., L. Yue, and D. Clapham. 2002. The TRPM7 channel is inactivated by PIP_2 hydrolysis. *Nat. Cell Biol.* 4:329–336.

Salkoff, L., A. Butler, G. Ferreira, C. Santi, and A. Wei. 2006. High-conductance potassium channels of the SLO family. *Nat. Rev. Neurosci.* 7:921–931.

Shyng, S.L., C. Cukras, J. Harwood, and C. Nichols. 2000. Structural determinants of PIP_2 regulation of inward rectifier K(ATP) channels. *J. Gen. Physiol.* 116:599–608.

Suh, B.C., and B. Hille. 2005. Regulation of ion channels by phosphatidylinositol 4,5-bisphosphate. *Curr. Opin. Neurobiol.* 15:370–378.

Suh, B.C., T. Inoue, T. Meyer, and B. Hille. 2006. Rapid chemically induced changes of PtdIns(4,5)P2 gate KCNQ ion channels. *Science.* 314:1454–1457.

Sun, X., D. Zhou, P. Zhang, E. Moczydlowski, and G. Haddad. 2007. β-Subunit-dependent modulation of hSlo BK current by arachidonic acid. *J. Neurophysiol.* 97:62–69.

Thebaud, B., E. Michelakis, X. Wu, R. Moudgil, M. Kuzyk, J. Dyck, G. Harry, K. Hashimoto, A. Haromy, I. Rebeyka, and S. Archer. 2004.

Oxygen-sensitive Kv channel gene transfer confers oxygen responsiveness to preterm rabbit and remodeled human ductus arteriosus: implications for infants with patent ductus arteriosus. *Circulation*. 110:1372–1379.

Tolloczko, B., S. Choudry, S. Bisotto, E. Fixman, and J. Martin. 2002. Src modulates serotonin-induced calcium signaling by regulating phosphatidylinositol 4,5-bisphosphate. *Am. J. Physiol. Lung Cell Mol. Physiol.* 282:L1305–L1313.

Voets, T., and B. Nilius. 2007. Modulation of TRPs by PIPs. *J. Physiol.* 582:939–944.

Wang, B., and R. Brenner. 2006. An S6 mutation in BK channels reveals β1 subunit effects on intrinsic and voltage-dependent gating. *J. Gen. Physiol.* 128:731–744.

Weiger, T., A. Hermann, and I. Levitan. 2002. Modulation of calcium-activated potassium channels. *J. Comp. Physiol. A Neuroethol. Sens. Neural. Behav. Physiol.* 188:79–87.

Wilkerson, M.K., T.J. Heppner, A.D. Bonev, and M.T. Nelson. 2006. Inositol trisphosphate receptor calcium release is required for cerebral artery smooth muscle cell proliferation. *Am. J. Physiol. Heart Circ. Physiol.* 290:H240–H247.

Xie, J., and D.P. McCobb. 1998. Control of alternative splicing of potassium channels by stress hormones. *Science*. 280:443–446.

Yaradanakul, A., S. Feng, C. Shen, V. Lariccia, M. Lin, J. Yang, T. Kang, P. Dong, H. Yin, J. Albanesi, and D. Hilgemann. 2007. Dual control of cardiac Na^+ Ca^{2+} exchange by PIP_2: electrophysiological analysis of direct and indirect mechanisms. *J. Physiol.* 582:991–1010.